

Variable Energy Photoelectron Spectroscopy: Periodic Trends in d-Orbital Energies for Organometallic Compounds of the Transition Metals

XIAORONG LI,[†] G. M. BANCROFT,^{*,†,‡} AND R. J. PUDDEPHATT^{*,†}

Department of Chemistry, The University of Western Ontario, London, Canada N6A 5B7, and Canadian Synchrotron Radiation Facility, Synchrotron Radiation Centre, University of Wisconsin—Madison, Stoughton, Wisconsin 53589

Received November 20, 1996

Introduction

Molecular photoelectron spectroscopy (PE) came into prominence with the studies of Turner and his co-workers in the early 1960s.¹ It was shown that when a photon beam irradiates a molecule, and if the photon energy ($h\nu$) is larger than the binding energy (E_b or BE) of a molecular orbital (MO), the electrons in that MO will be ejected. On the basis of the relationship $h\nu = E_b + E_k$ a photoelectron spectrometer sorts the binding energies of molecular orbitals according to the different kinetic energies (E_k) of the outgoing electrons. Usually, in the outer valence levels of an organometallic molecule, there is a one-to-one correspondence between the binding energies and molecular orbital energies (Koopmans' theorem). Therefore,

Xiaorong Li was born in Xian, Shaanxi Province, China. He obtained his B.Sc. from Shaanxi Normal University in 1982, his M.Sc. degree from Shanxi University in 1988. After three years as a lecturer in the Department of Chemistry, Shaanxi Normal University, he came to the University of Western Ontario in 1991. He completed his Ph.D. on photoelectron spectroscopy of organometallics in 1995, and took up a postdoctorate fellowship in the Department of Chemistry, University of Calgary.

G. M. Bancroft received his B.Sc. (Honors) (1963) and M.Sc. (1964) at the University of Manitoba. He then obtained his Ph.D. (1967) and D.Sc. (1979) from the University of Cambridge. After three years on faculty at the University of Cambridge, he returned to the University of Western Ontario in London, Canada, in 1970. He was appointed Professor in 1974, and was Chair of the department between 1986 and 1991 and between 1992 and 1995. His research has focused on the development and uses of several forms of high-energy spectroscopy: Mossbauer spectroscopy, photoelectron spectroscopy, and spectroscopies (XANES, Auger, photoelectron) using synchrotron radiation. He has been Scientific Director of the Canadian Synchrotron Radiation Facility (since 1981) at the Aladdin synchrotron and President of the Canadian Institute of Synchrotron (since 1991) which has been promoting a synchrotron in Canada.

R. J. Puddephatt was educated at University College London, graduating with a B.Sc. in chemistry in 1965 and Ph.D. in 1968 for research in organotin and organolead chemistry carried out with A. G. Davies and R. J. H. Clark. After two years as postdoctoral fellow with H. C. Clark at the University of Western Ontario, he was appointed lecturer at the University of Liverpool. He returned to the University of Western Ontario as professor in 1978. His interests are in organometallic and coordination chemistry of the late transition elements, with relevance to applications in catalysis and materials science. In catalysis, he has contributed to mechanistic studies of bond activation by oxidative addition and the modeling of surface reactivity by coordinatively unsaturated clusters, while in materials chemistry his research ranges from chemical vapor deposition to the synthesis of organometallics polymers and dendrimers.

photoelectron spectroscopy is the most direct way to probe the orbital ordering of molecules.

What kind of information can we get from the photoelectron spectra of a molecule if these spectra are recorded at different photon energies? It was recognized early on by Price² that the binding energies provided by a photoelectron spectrum are independent of the photon energy employed, but band intensities (photoionization cross sections) vary with photon energy. The band intensity variations as a function of photon energy can disclose important information on the orbital origin of the ejected electrons. In his pioneering work, Price used He I (21.2 eV) and He II (40.8 eV) photons to explore the correlation between band intensity and photon energy.

Synchrotron radiation provides the intense tunable source of photons needed to study the continuous variation of atomic and molecular photoionization cross sections with photon energy. The increasing availability of this radiation, coupled with the advent of high-resolution electron spectrometers, has greatly enhanced our ability to make orbital assignments for PE spectra.³

Only in the last nine years (starting in 1987) has variable energy photoelectron spectroscopy been applied to organometallics, including $M(\text{CO})_6$ ($M = \text{Cr}, \text{Mo}, \text{W}$),⁴ $M(\eta^5\text{-C}_5\text{H}_5)_2$ ($M = \text{Fe}, \text{Ru}, \text{Os}$),⁵ $\text{U}(\eta^8\text{-C}_8\text{H}_8)_2$,⁶ $(\eta^5\text{-C}_5\text{H}_5)\text{PtMe}_3$,⁷ $(\eta^7\text{-C}_7\text{H}_7)\text{M}(\eta^5\text{-C}_5\text{H}_5)$ ($M = \text{Ti}, \text{Nb}, \text{Mo}$),⁸ $(\eta^7\text{-C}_7\text{H}_7)\text{Ta}(\eta^5\text{-C}_5\text{H}_4\text{Me})$,⁸ $\text{Cr}(\eta^6\text{-C}_6\text{H}_6)_2$,⁹ $\text{Mo}(\eta^6\text{-C}_6\text{H}_5\text{Me})_2$,⁹ $\text{M}(\eta^5\text{-C}_5\text{H}_5)_2$ ($M = \text{V}, \text{Cr}, \text{Co}, \text{Ni}$),¹⁰ and $[(\eta^5\text{-C}_5\text{H}_4\text{iPr})\text{MoS}]_4$,¹¹ and it has been shown that the information content from a PE experiment is greatly enhanced in such studies. The merits of using synchrotron radiation to study the PE spectra of these molecules have been well documented by Green.³ However, prior to our work, variable energy photoelectron studies, along with related theoretical developments on photoionization cross sections, have not been reported for systematic studies of organometallic compounds of the late transition metals. For some important organometallic molecules of these metals, such as $M(\eta^3\text{-C}_3\text{H}_3)_2$ ($M = \text{Ni}, \text{Pd}, \text{Pt}$), the MO ordering assigned from photoelectron spectra and theoretical calculations has been very controversial.¹² The sharp difference of cross section behavior between the ligand orbital ionizations and metal d ioniza-

[†] The University of Western Ontario.

[‡] University of Wisconsin—Madison.

- (1) Turner, D. W.; Baker, A. D.; Baker, C.; Brundle, C. R. *Molecular Photoelectron Spectroscopy: A Handbook of He 584 Å Spectra*; Wiley-Interscience: New York, 1970.
- (2) Price, W. C.; Potts, A. W.; Streets, D. G. In *Electron Spectroscopy*; Shirley, D. A., Ed.; North-Holland: Amsterdam, 1972.
- (3) Green, J. C. *Acc. Chem. Res.* **1994**, *27*, 131.
- (4) Cooper, G.; Green, J. C.; Payne, M. P.; Dobson, B. R.; Hillier, I. H. *J. Am. Chem. Soc.* **1987**, *109*, 3836.
- (5) Cooper, G.; Green, J. C.; Payne, M. P. *Mol. Phys.* **1988**, *63*, 1031.
- (6) Brennan, J. G.; Green, J. C.; Redfern, C. M. *J. Am. Chem. Soc.* **1989**, *111*, 2373.
- (7) Yang, D. S.; Bancroft, G. M.; Puddephatt, R. J.; Tan, K. H.; Cutler, J. N.; Bozek, J. B. *Inorg. Chem.* **1990**, *29*, 4956.
- (8) Green, J. C.; Kaltsoyannis, N.; Sze, K. H.; MacDonald, M. *J. Am. Chem. Soc.* **1994**, *116*, 1994.
- (9) Brennan, J. G.; Cooper, G.; Green, J. C.; Kaltsoyannis, N.; MacDonald, M. A.; Payne, M. P.; Redfern, C. M.; Sze, K. H. *Chem. Phys.* **1992**, *164*, 271.
- (10) Brennan, J.; Cooper, G.; Green, J. C.; Payne, M. P.; Redfern, C. M. *J. Electron Spectrosc. Relat. Phenom.* **1993**, *66*, 101.
- (11) Davis, C. E.; Green, J. C.; Kaltsoyannis, N.; MacDonald, M. A.; Qin, J.; Rauchfuss, T. B.; Redfern, C. M.; Stringer, G. H.; Woolhouse, M. G. *Inorg. Chem.* **1992**, *31*, 3779.

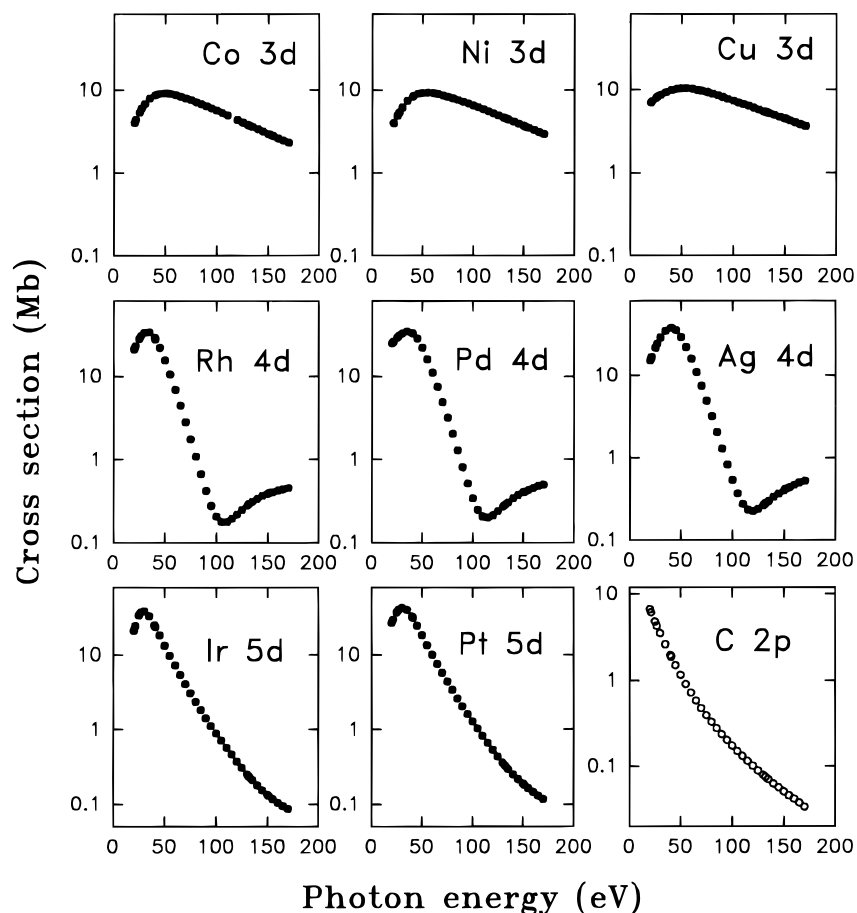


FIGURE 1. Theoretical photoionization cross sections of metal d and C 2p orbitals.¹³

tions made it possible for us to use synchrotron radiation to reassign the MO ordering of these molecules, and thus enabled us to reveal periodic trends in the molecular orbital energies of these molecules. These periodic trends, which have not been reviewed in the literature, will be summarized in this Account.

MO Assignments of Photoelectron Spectra Using Band Intensity Variations

With variable energy photoelectron spectroscopy, we monitor the photoelectron band intensities as a function of photon energy, usually between ~ 20 and ~ 150 eV. The relative band intensities vary because the atomic cross sections (and thus the molecular orbital cross sections) have very different trends with photon energy. For example, Figure 1 shows the theoretical cross sections as a function of photon energy (from 20 to 170 eV) for the carbon 2p and d orbitals of the late transition metals. These atomic orbitals form the major components of the outer valence region of organometallic molecules.¹³ Obviously, the cross section trends for the metal d and C 2p orbitals are very different. For example, the C 2p cross sections (along with other common ligand orbital cross sections such as N 2p and O 2p) show a rapid monotonic decay above the threshold. In contrast, the metal d cross sections all show an initial increase in cross section above the threshold (so-called delayed maxima), followed by a

decrease. The rate of decrease in cross section is much smaller for the first-row transition metals compared to the second- and third-row metals, while the second-row metal 4d cross section goes through a minimum (Cooper minimum) at >100 eV.

A model (so-called Gelius model¹⁴) which is important for variable energy photoelectron spectroscopy states that *the trend of photoionization cross sections as a function of photon energy for a molecular orbital is mainly determined by that of its predominant atomic orbital components.*¹⁴ For organometallic compounds, the cross section variation of nonbonding metal d and ligand carbon 2p orbitals should behave like their atomic counterparts, and those of the bonding MOs behave in an intermediate manner. This statement is more reliable quantitatively when the photon energy is large (>50 eV), and when the magnitude of one atomic orbital cross section is dominant over all the other atomic orbital contributions.¹⁵ This rule has been successfully applied in our variable energy photoelectron spectroscopic studies of organometallic compounds of the late transition metals, such as $M(\eta^3\text{-C}_3\text{H}_5)_2$ ($M = \text{Ni, Pd, Pt}$).¹⁶ The above study was particularly successful because there are a few “nonbonding” ligand

(12) Li, X.; Bancroft, G. M.; Puddephatt, R. J.; Hu, Y. F.; Liu, Z. F.; Tan, K. H. *Inorg. Chem.* **1992**, *31*, 5162.

(13) Yeh, J. J.; Lindau, I. *At. Nucl. Data Tables* **1985**, *32*, 1.

(14) (a) Gelius, U. In *Electron Spectroscopy*; Shirley, D. A., Ed.; North-Holland: Amsterdam, 1972; p 311. (b) Bancroft, G. M.; Malmquist, P.-A.; Svensson, S.; Basilier, E.; Gelius, U.; Siegbahn, K. *Inorg. Chem.* **1978**, *17*, 1595.

(15) Kono, S.; Kobayashi, T. *Solid State Commun.* **1974**, *15*, 1421.

(16) Li, X.; Bancroft, G. M.; Puddephatt, R. J.; Liu, Z. F.; Hu, Y. F.; Tan, K. H. *J. Am. Chem. Soc.* **1994**, *116*, 9543.

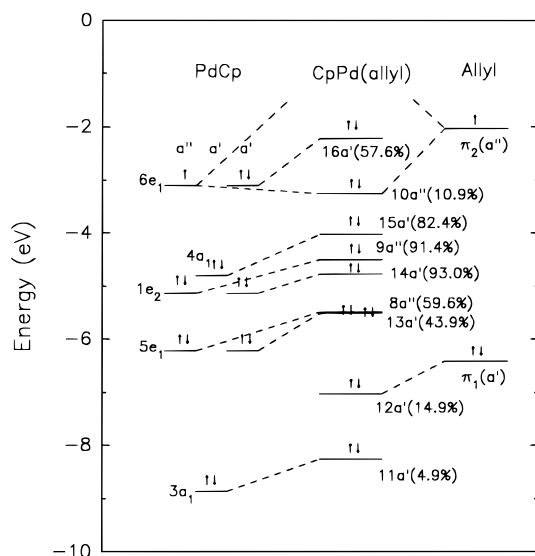


FIGURE 2. X α -SW MO diagrams for the formation of the outer valence of $(\eta^5\text{-C}_5\text{H}_5)\text{Pd}(\eta^3\text{-C}_3\text{H}_5)$. The Pd 4d compositions are put beside the MOs of $(\eta^5\text{-C}_5\text{H}_5)\text{Pd}(\eta^3\text{-C}_3\text{H}_5)$.

and metal d orbitals in the outer valence of these molecules, which makes the intensity changes of many bands in the low binding energy region behave like atomic metal d and carbon 2p orbitals. The sharp difference in the trends of cross section between metal d and ligand orbitals (Figure 1) allow us to assign these PE spectra with confidence. The above cross section rule is also supported by X α -SW cross section calculations for MOs for $\text{M}(\eta^5\text{-C}_5\text{H}_5)_2$.¹⁶ The calculations indeed show that the nonbonding MOs behave like their atomic counterparts, and bonding MOs show intermediate behavior.

To illustrate the power of the variable energy approach, we look first at the PE spectrum of $(\eta^5\text{-C}_5\text{H}_5)\text{Pd}(\eta^3\text{-C}_3\text{H}_5)$.¹⁷ The reasons for us to use this molecule as an example are (1) the bands in the outer valence of its PE spectrum are well resolved, so the one-to-one relationship between photoelectron bands and molecular orbitals can be best seen; (2) there is a fairly broad distribution of metal d compositions among the MOs in the outer valence region, *i.e.*, some MOs are Pd 4d based, some are mainly bonding MOs between Pd 4d and Cp, some are nonbonding Cp π_1 and allyl π_1 , and one MO is from bonding between PdCp and allyl. The sequence of Pd percent compositions for these MOs is Pd 4d based > Pd-Cp bonding > Pd-Cp-allyl bonding and π_1 MOs of allyl and Cp. This variation of metal d compositions has been disclosed very clearly by the different degrees of band intensity variations observed from the variable energy photoelectron spectra of this molecule.

Figure 2 shows a X α -SW MO diagram showing the formation of the MOs of $(\eta^5\text{-C}_5\text{H}_5)\text{Pd}(\eta^3\text{-C}_3\text{H}_5)$ between PdCp and allyl fragments. The calculated Pd 4d compositions are shown beside each orbital. Among the nine occupied orbitals in the outer valence region, there are three orbitals (15a', 9a'', and 14a') whose Pd 4d compositions are >82%. They are designated the Pd 4d based MOs. These MOs are located in the middle part of the outer valence region. Among other MOs, there are three

PdCp based MOs (16a', 8a'', and 13a'). These MOs are bonding orbitals formed by interaction between Pd 4d and Cp π_2 orbitals, and their Pd 4d compositions are in the intermediate range, between 44% and 60%. The 10a'' orbital is the only bonding MO formed by interaction between PdCp and allyl orbitals whose Pd 4d composition (10.9%) is more diluted by mixing with ligand carbon 2p orbitals from both Cp and allyl π_2 orbitals. The Pd 4d compositions of 12a' and 11a' are 14.9% and 4.9%, respectively. They are mainly allyl π_1 and Cp π_1 orbitals, respectively. The MO diagram shows that on the low BE side of the three Pd 4d based MOs, there are two MOs: one is the HOMO which is one of the PdCp based MOs, (10a''); the other (15a') is the bonding MO between PdCp and allyl. On the high BE side of the three Pd 4d based MOs, two PdCp MOs (8a'', 13a') are located closely, and two ligand π_1 MOs (12a', 11a'') are at higher BE.

The above orbital ordering is confirmed by the variable energy photoelectron spectra of $(\eta^5\text{-C}_5\text{H}_5)\text{Pd}(\eta^3\text{-C}_3\text{H}_5)$ (Figure 3) recorded at 21.2, 40, 50, and 60 eV, respectively, covering the photon energy range in which the Pd 4d delayed maximum takes major effect. The spectra display eight bands corresponding to the first eight MOs in the outer valence region. The three bands (bands 3, 4, and 5) in the middle binding energy region increase in intensity with an increase in photon energy. They are assigned to the three Pd 4d based orbitals, as predicted from the MO diagram and the Gelius model. All other bands decrease in relative intensity, with bands 2 and 8 decreasing more than bands 1, 6, and 7. Therefore, it is reasonable to assign bands 2 and 8 to the MOs with the smallest Pd 4d character (band 2 to 10a'' and band 8 to 12a'), and bands 1, 6, and 7 must be assigned to the three MOs with intermediate Pd 4d character (16a', 8a'', and 13a', respectively).

In the $(\eta^5\text{-C}_5\text{H}_5)\text{Pd}(\eta^3\text{-C}_3\text{H}_5)$ case, the calculated orbital ordering is in agreement with that deduced from the variable energy spectra, and the ratios of intensity variation for each band are also consistent with the relative Pd 4d compositions calculated with the X α -SW method, strongly suggesting that the Gelius model has semiquantitative significance for MOs of variable Pd 4d composition. The variable energy technique, combined with MO calculations, is obviously a powerful method to confirm MO assignments.

Although the traditional He I (21.2 eV)/He II (40.8 eV) ratio of band intensity can help to assign PE spectra for some organometallic compounds, the low-energy and noncontinuous feature of helium light limits its usefulness. For example, in our studies for PE spectra of copper(I) β -diketonate complexes,¹⁸ we noticed that the mainly Cu 3d band cannot be assigned unambiguously by using the He I/He II intensity ratio. The Cu 3d band only shows the expected large increase in relative intensity above 40.8 eV (He II radiation). Only by taking spectra above 50 eV does the Cu 3d band assignment become very obvious.

It is also important to emphasize that, often, the energy ordering determined by the variable energy technique

(17) Li, X.; Tse, J. S.; Bancroft, G. M.; Puddephatt, R. J. *Organometallics* **1995**, *14*, 4513.

(18) Li, X.; Bancroft, G. M.; Puddephatt, R. J.; Yuan, Z.; Tan, K. H. *Inorg. Chem.* **1996**, *35*, 5040.

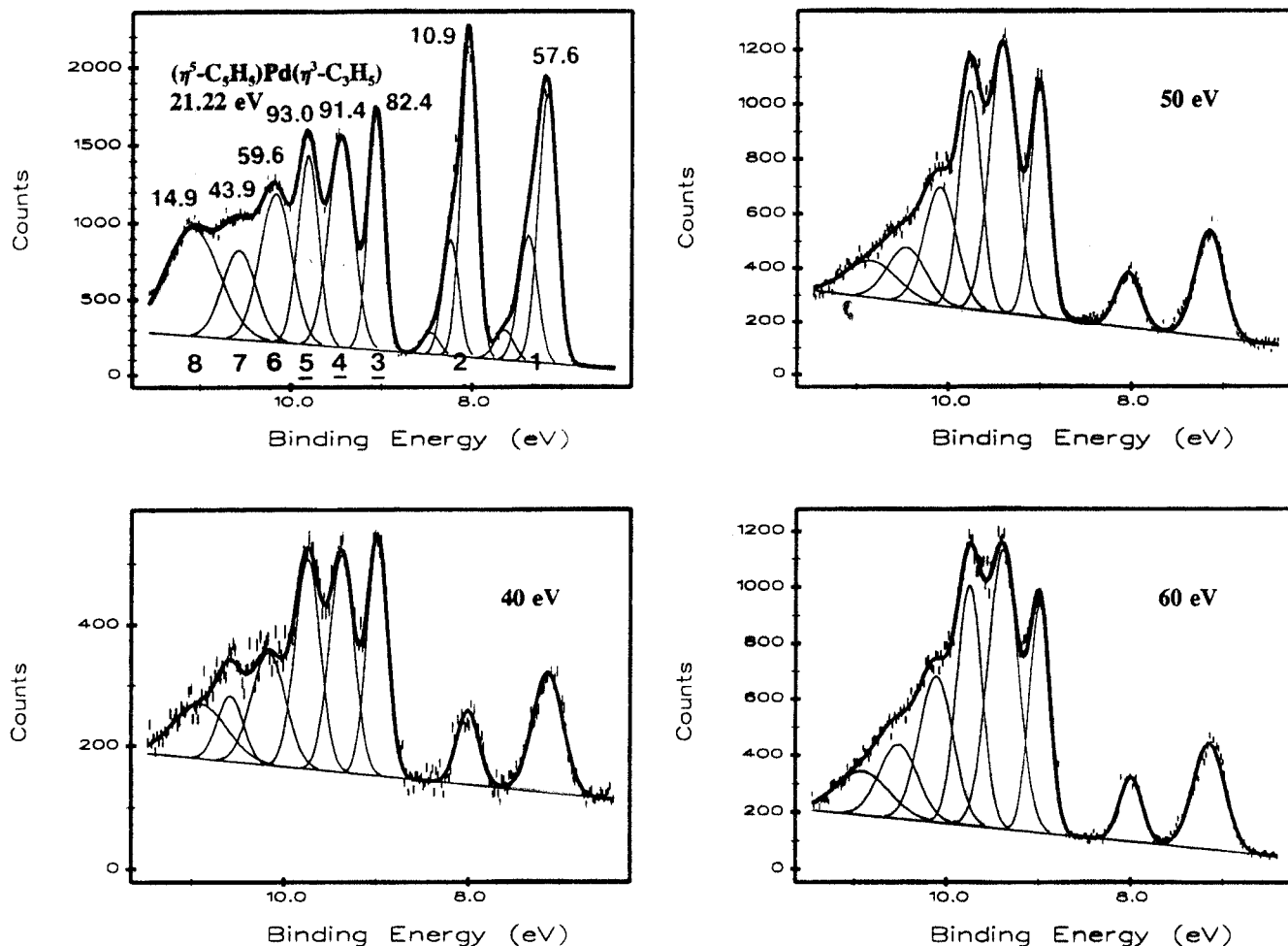


FIGURE 3. Representative variable energy photoelectron spectra of $(\eta^5\text{-C}_5\text{H}_5)\text{Pd}(\eta^3\text{-C}_3\text{H}_5)$ recorded at 21.22, 40, 50, and 60 eV. The $X\alpha$ -SW Pd 4d compositions (%) are given at the top of each band. Band numbers are at the bottom with the Pd 4d based bands underlined.

does not agree with the ordering from MO calculations. For example, for $\text{Ni}(\eta^3\text{-C}_3\text{H}_5)_2$, the orbital ordering did not agree with the ordering from any theoretical calculation—either our $X\alpha$ -SW calculation or many others!¹⁶ The variable energy method seems much more reliable than MO calculations for transition metal complexes.

Periodic Trends

To determine periodic trends in metal d orbital energies, it is highly desirable to have volatile gas phase analogues for a given transition metal group available, because the PE resolution in the gas phase is generally much better than for solid state spectra. Fortunately, stable volatile analogues are now available, and the cross section variations described above make it rather easy to identify the metal d levels.

General trends in metal d energies can be seen immediately by looking at a few spectra. For the early transition metal organometallic compounds, the PE spectra down a group are very similar. For example, the He I spectra of $\text{M}(\text{CO})_6$ molecules ($\text{M} = \text{Cr}, \text{Mo}, \text{W}$)¹⁹ are shown in Figure 4. These spectra are qualitatively very similar, and even the metal d energies vary only by 0.16 eV from $\text{Cr}(\text{CO})_6$ to $\text{W}(\text{CO})_6$. If we now go to the next group (Figure

5), the spectra of $\text{CpM}(\text{CO})_3$ analogues ($\text{M} = \text{Mn}, \text{Re}$)²⁰ are still qualitatively similar, but the metal d energies now differ by ~ 0.34 eV. In contrast, when we turn to the spectra of organometallic compounds of the later transition metals, some striking differences occur. Figure 6 shows the outer valence PE spectra of $\text{M}(\eta^3\text{-C}_3\text{H}_5)_2$ ($\text{M} = \text{Ni}, \text{Pd}, \text{Pt}$)¹⁶ and $\text{CpM}(\text{CO})_2$ ($\text{M} = \text{Co}, \text{Rh}, \text{Ir}$)²¹ all recorded with He I photons. It is immediately apparent that the spectra of the first-row Ni and Co complexes differ greatly from the spectra of the second- and third-row analogues. For example, the $\text{Ni}(\eta^3\text{-C}_3\text{H}_5)_2$ spectrum shows three resolvable peaks at 8 ± 0.4 eV BE, whereas the Pd and Pt analogues only show one peak in this region. But at higher binding energy (8.5–12 eV), there are many more peaks in the Pd and Pt spectra than in the Ni analogue. The variable energy spectra (Figure 7) show that peak 1 in the spectra of $\text{Pd}(\eta^3\text{-C}_3\text{H}_5)_2$ must be due to a mainly ligand orbital because the intensity of peak 1 decreases from 24 to 80 eV photon energy. In contrast, peaks 1 and 2 for $\text{Ni}(\eta^3\text{-C}_3\text{H}_5)_2$ must be due mainly to Ni 3d orbitals because their intensity increases with photon energy. Thus, the Ni 3d orbitals must have a ≥ 1 eV lower BE than the Pd 4d BE for the Pd analogue.

(19) (a) Higginson, B. R.; Lloyd, D. R.; Connor, J. A.; Hillier, I. H. *J. Chem. Soc., Faraday Trans. 2* **1974**, *70*, 1418. (b) Cowley, A. H. *Prog. Inorg. Chem.* **1979**, *26*, 46.

(20) (a) Hu, Y. F.; Bancroft, G. M.; Liu, Z. F.; Tan, K. H. *Inorg. Chem.* **1995**, *34*, 3716. (b) Calabro, D. C.; Hubbard, J. L.; Blevins II, C. H.; Andrew, C. C.; Lichtenberger, D. L. *J. Am. Chem. Soc.* **1981**, *103*, 6839.

(21) Li, X.; Bancroft, G. M.; Puddephatt, R. J.; Hu, Y. F.; Tan, K. H. *Organometallics* **1996**, *15*, 2890.

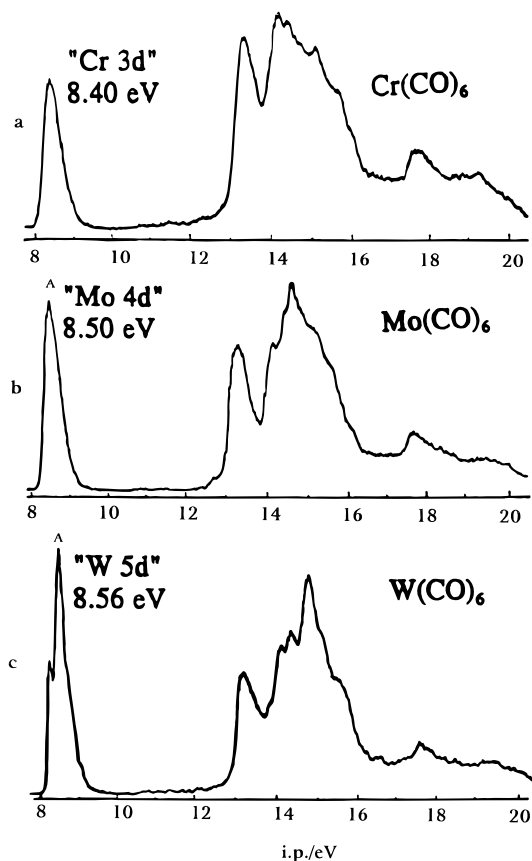


FIGURE 4. He I spectra of $M(\text{CO})_6$ ($M = \text{Cr, Mo, and W}$).^{19a} The metal nd ($n = 3, 4, 5$) bands and their binding energies are specified.

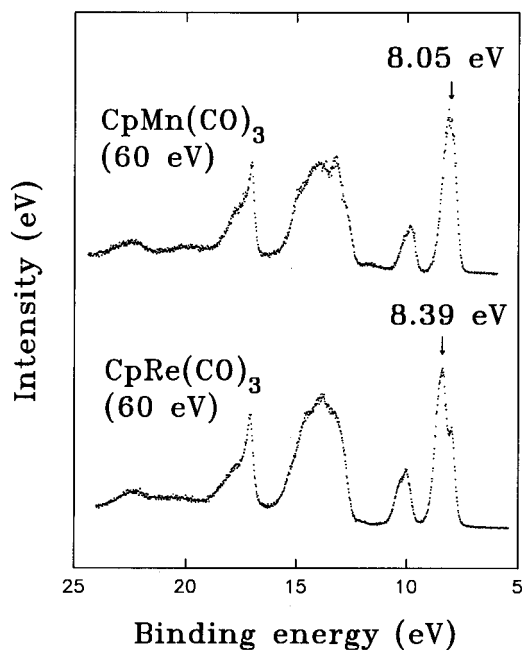


FIGURE 5. PE spectra of $(\eta^5\text{-C}_5\text{H}_5)\text{M}(\text{CO})_3$ ($M = \text{Mn and Re}$) recorded at 60 eV photon energy. The binding energies of metal 3d (Mn) and 5d (Re) based bands are specified.

It is also very important from Figure 6 that the second- and third-row spectra of analogues are very similar, with the spectra of $\text{Pt}(\eta^3\text{-C}_3\text{H}_5)_2$ and $\text{CpIr}(\text{CO})_2$ showing one more resolved peak than $\text{Pd}(\eta^3\text{-C}_3\text{H}_5)_2$ and $\text{CpRh}(\text{CO})_2$ respectively. Even the order of orbital assignments is the same, with the symmetry and character of orbitals in the second- and third-row complexes being identical. For

example, assignments of bands, 1, 2, 3, 4, 5, and 7 for $\text{Pd}(\eta^3\text{-C}_3\text{H}_5)_2$ are the same as these from bands 1, 2, 3, 4, 5, and 8 for $\text{Pt}(\eta^3\text{-C}_3\text{H}_5)_2$. Band 6 of $\text{Pd}(\eta^3\text{-C}_3\text{H}_5)_2$ is broad and contains two MOs corresponding to bands 6 and 7 of $\text{Pt}(\eta^3\text{-C}_3\text{H}_5)_2$.

From the above discussion, the qualitative differences in spectra are due mainly to the shift in Ni 3d and Co 3d binding energies to much lower values. Indeed, the ligand based orbitals, such as bands 5 and 6 for $\text{Ni}(\eta^3\text{-C}_3\text{H}_5)_2$, have a BE very similar to those of the corresponding ligand orbitals in the Pd (bands 6 and 7) and Pt (bands 7 and 8) analogues.

The orbital sequences for the three compounds from the variable energy technique can now be summarized (with the band number in parentheses and the main character of the MO—either metal (M) or ligand (L)—following). $\text{Ni}(\eta^3\text{-C}_3\text{H}_5)_2$: $13a_g$ (1, M) < $12a_g$ (1, M) < $6b_g$ (2, M) < $7a_u$ (2, L) < $11a_g$ (3, M) < $5b_g$ (4, M) < $11b_u$ (5, L) < $10a_g$ (6, L). $\text{Pd}(\eta^3\text{-C}_3\text{H}_5)_2$: $8a_u$ (1, L) < $17a_g$ (2, M) < $16a_g$ (3, M) < $8b_g$ (4, M) < $15a_g$ (5, M) < $7b_g$ (6, M) < $13b_u$ (6, L) < $14a_g$ (7, L). $\text{Pt}(\eta^3\text{-C}_3\text{H}_5)_2$: $12a_u$ (1, L) < $21a_g$ (2, M) < $20a_g$ (3, M) < $10b_g$ (4, M) < $19a_g$ (5, M) < $9b_g$ (6, M) < $19b_u$ (7, L) < $18a_g$ (8, L). From the spectra in Figures 4–6, it is apparent that the average binding energy difference (ΔE_b) between metal 3d (first-row) and 4d (second-row) orbitals is much larger for the late transition metals than the early transition metals. The sequence of ΔE_b is $\text{M}(\text{CO})_6$ ($M = \text{Cr and Mo, } 0.10 \text{ eV}$)¹⁹ < $\text{CpM}(\text{CO})_3$ ($M = \text{Mn and Re, } 0.34 \text{ eV}$)²⁰ < MCp_2 ($M = \text{Fe and Ru, } 0.59 \text{ eV}$)²² < $\text{CpM}(\text{CO})_2$ ($M = \text{Co and Rh, } 0.71 \text{ eV}$)²¹ < $\text{M}(\eta^3\text{-C}_3\text{H}_5)_2$ ($M = \text{Ni and Pd, } 1.17 \text{ eV}$)¹⁶ < $(\text{hfac})\text{MPMe}_3$ ($M = \text{Cu and Ag, hfac} = \text{CF}_3\text{C}(\text{O})\text{CHC}(\text{O})\text{CF}_3, 1.9 \text{ eV}$).¹⁸

Origin of the Difference in Metal d Ionizations

What is the reason for this trend, in which the energy difference between 3d and 4d or 5d orbitals for analogous compounds appears to increase for the later transition metals? Lichtenberger *et al.*^{23,24} attributed the d binding energy separation in $\text{CpM}(\text{CO})_2$ ($M = \text{Co and Rh}$) mainly to the larger relaxation energy associated with first-row complexes. The orbital relaxation effect is mainly due to the orbital contraction on ionization. This effect makes the ion state more stable relatively, and lowers the BE. On the other hand, Ziegler *et al.*²⁵ proposed that trends in the thermal stability and kinetic lability of the metal–carbonyl bond in $\text{M}(\text{CO})_6$ ($M = \text{Cr, Mo, and W}$), $\text{M}(\text{CO})_5$ ($M = \text{Fe, Ru, and Os}$), and $\text{M}(\text{CO})_4$ ($M = \text{Ni, Pd, and Pt}$) were due to the ground state energy differences between the first- and second- or third-row transition metals. They suggested that, in the ground state, the 4d and 5d metal orbitals are lower in energy (higher in BE) than the 3d orbitals, since d–d repulsions are smaller for the diffuse 4d and 5d orbitals than for the contracted 3d orbitals and that this difference should increase from the early to the

- (22) (a) $\text{Fe}(\eta^5\text{-C}_5\text{H}_5)_2$: Rabalais, J. W.; Werme, L. O.; Bergmark, T.; Karlsson, L.; Hussain, M.; Siegbahn, K. *J. Chem. Phys.* **1972**, *57*, 1185. (b) $\text{Ru}(\eta^5\text{-C}_5\text{H}_5)_2$: Evans, S.; Green, M. L. H.; Jewitt, B.; Orchard, A. F.; Pygall, C. F. *J. Chem. Soc., Faraday Trans. 2* **1972**, *68*, 1847.
 (23) Lichtenberger, D. L.; Calabro, D. C.; Kellogg, G. E. *Organometallics* **1984**, *3*, 1623.
 (24) (a) Calabro, D. C.; Lichtenberger, D. L. *Inorg. Chem.* **1980**, *19*, 1732. (b) Lichtenberger, D. L.; Kellogg, G. E. *Acc. Chem. Res.* **1987**, *20*, 379.
 (25) Ziegler, T.; Tschinke, V.; Ursenbach, C. *J. Am. Chem. Soc.* **1987**, *109*, 4825.

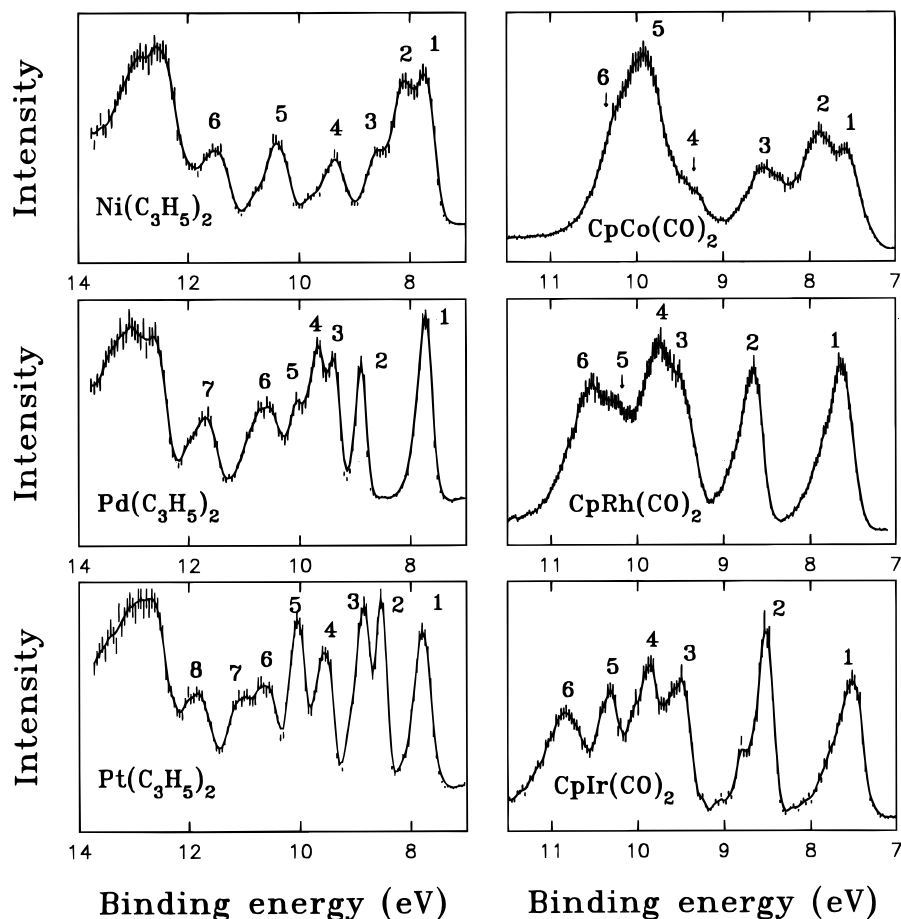


FIGURE 6. He I spectra of $M(\eta^3\text{-C}_3\text{H}_5)_2$ ($M = \text{Ni, Pd, and Pt}$) and $(\eta^5\text{-C}_5\text{H}_5)M(\text{CO})_2$ ($M = \text{Co, Rh, and Ir}$).

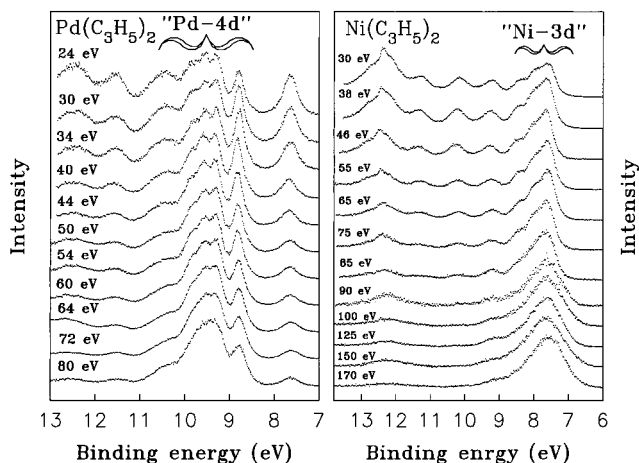


FIGURE 7. Band intensity increase with photon energy for Pd 4d and Ni 3d based bands in the spectra of $M(\eta^3\text{-C}_3\text{H}_5)_2$ ($M = \text{Ni and Pd}$). The photon energy range for the Pd compound is covering that for the Pd 4d delayed maximum.

late transition metals. Due to the "lanthanide contraction", the energies of 4d and 5d metal orbitals are relatively close. The X α calculations carried out for $\text{CpM}(\text{CO})_2$ ($M = \text{Co, Rh, and Ir}$)²¹ and $M(\eta^3\text{-C}_3\text{H}_5)_2$ ($M = \text{Ni, Pd, and Pt}$)¹⁶ in our work support Ziegler's interpretation in terms of the difference in ground state d orbital energies. It is also supported by the difference in slopes among experimental curves of relative band intensity variation (branching ratio) for the HOMOs of $\text{CpM}(\text{CO})_2$ ($M = \text{Co, Rh, and Ir}$).²¹ The HOMOs of these molecules are the antibonding orbitals from the interaction of $\text{M}(\text{CO})_2$ with Cp. The slope

difference suggests that the HOMO of the Co compound has more metal d character than those of the Rh and Ir analogues, thus supporting the ground-state d BE energy sequence 3d (Co) < 4d (Rh) \approx 5d (Ir).

Concluding Remarks

The large metal d binding energy difference between the first and second or third late transition rows has been confirmed by variable energy photoelectron spectroscopy. Its origin, most likely a ground-state d energy difference, may help us to understand some special features associated with the late transition metals, such as the relative σ and π bonding between metal and carbonyl ligands,²¹ and the very different reactions of olefins on Ni versus Pt surfaces (which may be largely due to the enhanced metal-olefin π bonding on Ni surfaces).^{26,27} The periodic trends of d energy separations for the late transition metals should be one of the essential factors for comprehending the different types of chemical reactions and catalytic processes associated with these metals.

We express our thanks to Zhifeng Liu, John Tse, Yongfeng Hu, Kim H. Tan, Jianzhang Xiong, Zhanfeng Yin, Jeff Cutler, and Doug Sutherland for their help. We also thank NSERC (Canada) for financial support and the staff at the Aladdin Synchrotron for continued assistance. We acknowledge the NSF for Grant No. DMR-9212658 to the Synchrotron Radiation Centre.

AR960277X

(26) Hammer, L.; Muller, K. *Prog. Surf. Sci.* **1991**, 103.

(27) Avery, N. R.; Sheppard, N. *Proc. R. Soc. London, A* **1986**, 405, 1, 27.